

Bioacoustics and molecular genetics reveal a new species of glassfrog, genus *Chimerella* (Anura: Centrolenidae), from white sand outcrops in the Yungas ecoregion of northeastern Peru

Pablo J. Venegas^{1,2}, Luis A. García-Ayachi^{1,2}, Jörn Köhler³ & Miguel Vences⁴

¹Rainforest Partnership, 4005 Guadalupe St., Austin, TX 78751, USA
²Instituto Peruano de Herpetología (IPH), Augusto Salazar Bondy 136, Urb. Higuereta, Surco, Lima, Peru
³Hessisches Landesmuseum Darmstadt, Friedensplatz 1, 64283 Darmstadt, Germany
⁴Zoological Institute, Technische Universität Braunschweig, Mendelssohnstr. 4, 38106 Braunschweig, Germany

Corresponding author: Pablo J. Venegas, ORCID 0000-0002-6501-4492, e-mail: pablo@rainforestpartnership.org

Manuscript received: 18 July 2025 Accepted: 16 October 2025 by LISA SCHULTE

Abstract. Based on molecular genetics, bioacoustics, and morphological comparisons, we provide independent lines of evidence for the recognition and description of a new species of *Chimerella* from the Amazonian slopes of the eastern Andes in northeastern Peru, departments of Amazonas and San Martín. *Chimerella zoeterra* sp. n. is distinguished from *C. corleone* and *C. mira* by exhibiting a light yellow-green dorsum covered with dark green punctuation and scattered black flecks in life, and the iris bearing an orange or grayish-red median streak. However, in life, the new species is morphologically indistinguishable from *C. mariaelenae*, differentiated from it only by the dorsal coloration in preservative (ethanol 70%): cream with a lavender hue in the new species and distinctly lavender in *C. mariaelenae*. The advertisement call of the new species differs from the calls of all other nominal *Chimerella* species by qualitative and quantitative character traits. Its call consists of 3 to 5 high-pitched, pulsed notes of 26–35 ms duration. Genetically, samples of the new species form a divergent mitochondrial lineage with uncorrected pairwise distances for the 16S rRNA gene of 2.3–4.2% to the other three nominal species of *Chimerella*. Furthermore, there is a lack of haplotype sharing with other nominal species in certain nuclear markers studied (RAG-1, KIAA 1239, and SACS). The new species inhabits riparian vegetation of black water streams in humid montane forest on white sand outcrops.

Key words. Amphibia, *Chimerella zoeterra* sp. n., *C. mariaelenae*, Marañón River, bioacoustics, molecular genetics, morphology, phylogeny, taxonomy.

Introduction

The tropical Andes region has the highest species richness, as well as the highest number and density of endemic animal and plant species among the global biodiversity hotspots (MYERS et al. 2000). Moreover, it is widely considered as one of the most threatened ecosystems globally (MYERS et al. 2000, MALCOLM et al. 2006, RODRIGUES et al. 2014). The Andes cover almost one third of the Peruvian territory from north to south with an altitudinal range between 1000 and 4000 m a.s.l. (Peñaherrera del Aguila 1989). Frogs are key to the importance of the Andes in the global pattern of biodiversity (Hutter et al. 2013). In fact, South America possesses the greatest species richness of frogs among continental regions, and the Andes contain more endemic frog species than any other region on

the continent, even more than twice the number of species known from the Amazon lowlands (Duellman 1999). As most Andean species have comparatively small ranges, the tropical Andes also have one of the greatest concentrations of threatened species of frogs (Luedtke et al. 2023).

The anuran family Centrolenidae, commonly known as glassfrogs, are a group of arboreal stream-breeding frogs famous for having completely or partially translucent venters. This Neotropical clade contains 167 species that were classified into 11 currently recognized genera (Ron et al. 2024, Frost 2025) and possesses its center of diversity and endemicity in the tropical Andes (Guayasamin et al. 2020). Currently, eight glassfrog genera are recognized in Peru: Centrolene, Chimerella, Cochranella, Hyalinobatrachium, Nymphargus, Rulyrana, Teratohyla, and Vitreorana (Frost 2025).

The genus Chimerella, on which our study focuses, is easily diagnosed from all other centrolenid genera by the combination of the following characters: presence of humeral spine in adult males, transparent ventral parietal peritoneum, and white pericardial, hepatic, and visceral peritonea (Guayasamin et al. 2020). To date, Chimerella contains three species restricted to the eastern Andean slopes and foothills of Ecuador and Peru (Fig. 1): C. mariaelenae (CISNEROS-HEREDIA & McDIARMID, 2006) from extreme northern Ecuador to extreme northern Peru in the Cordillera de Kampankis, at elevations between 813 and 1820 m a.s.l. (Catenazzi & Venegas 2012, Guayasamin et al. 2020, Köhler et al. 2023); C. corleone Twomey, Delia & Castroviejo-Fisher, 2014 known from two localities in the Cordillera Escalera in northeastern Peru, at elevations between 421 and 610 m a.s.l. (Twomey et al. 2014, Köhler et al. 2023); and C. mira KÖHLER, VENEGAS, CASTILLO-UR-BINA, GLAW, AGUILAR-PUNTRIANO & VENCES, 2023, a recently described species only known from its type locality in the Andean foothills of central Peru, at an elevation of 798 m a.s.l. (Köhler et al. 2023).

Over the two past decades, integrative taxonomy has become key for the discovery, recognition, and delimitation of species, especially for species complexes or species barely diagnosable by morphology alone, incorporating different sources of evidence to construct better justified species hypotheses (WILL et al. 2005, PADIAL et al. 2010, DALAPICOLLA & PERCEQUILLO 2020, VENCES et al. 2024a). The combination of molecular, morphological, and bioacoustic data has been instrumental in deciphering the limits and relationships within anuran species complexes, once considered to represent a single nominal taxon (e.g., PADIAL & DE LA RIVA 2009, FUNK et al. 2011, ORTEGA-AN-DRADE et al. 2015, PÁEZ & RON 2019, KÖHLER et al. 2024). Frequently, integrative taxonomy reveals deep evolutionary divisions among populations with a conservative morphology, difficult to diagnose by morphological traits alone (SITES & MARSHALL 2004).

In this study, using an integrative approach, we investigate populations of *Chimerella* from white sand outcrops in Yungas montane forests from the departments of Amazonas and San Martín, northwestern Peru, which are morphologically similar to *C. mariaelenae*, but phylogenetically and bioacoustically distinct.

Materials and methods

Field work

Specimens of *Chimerella* studied herein were collected during rapid herpetological inventories carried out in the departments of Amazonas and San Martín, northeastern Peru, between 2020 and 2023. The frogs were collected by hand via the complete species inventory technique (Scott 1994), during slow night walks (19:00 to 02:00 h) along streams and within the forest using headlamps. Collected specimens were anesthetized and euthanized with an overdose of 20% benzocaine gel applied on the ventral surfac-

es of individuals (McDiarmid 1994). Tissue samples were taken before fixation and stored in 96% ethanol, whereas specimens were fixed with formalin (10%) for 24 hours and subsequently stored in 70% ethanol. Voucher specimens are deposited in the herpetological collection of CORBIDI in Lima, Peru. Coordinates and elevation were taken with a Garmin GPS receiver (set to WGS84 datum).

Morphology

The terminology and definition of diagnostic characters follow Cisneros-Heredia & McDiarmid (2007) and GUAYASAMIN et al. (2020). The scheme of the description follows that of KÖHLER et al. (2023). Morphometric measurements were taken with a digital caliper and rounded to the nearest 0.1 mm. Measurements taken and used throughout the text are: SVL, snout-vent length; HL, head length (straight line distance from posterior corner of mouth to the tip of the snout); HW, head width (measured at level of angle of jaws); TD, tympanum diameter (measured horizontally); IND, internarial distance (straight line distance between the inner edge of the narial opening); IOD, interorbital distance (between anterior margins of orbits); ED, eye diameter (the horizontal length of orbit); EW, upper eyelid width (greatest transverse width of upper eyelid); END, eye-nostril distance (from anterior margin of orbit to center of nostril); HaL, hand length (from proximal edge of inner metacarpal tubercle to tip of third finger); TL, tibia length (taken with the flexed leg from the upper edge of knee to the lower edge of heel); THL, thigh length (from the middle of the cloacal slit to the proximal part of the femur-tibia articulation); FL, foot length (distance from proximal margin of inner metatarsal tubercle to tip of toe IV); and are provided in Table 1. Color in life was described using digital photographs. Specimens were sexed by dissection and visual inspection of the gonads. Specimens examined are listed in a table available at https://doi.org/10.5281/zenodo.14019863.

Bioacoustics

Vocalizations of the new species were recorded in the field using a digital recorder (Marantz PMD661 MK2) connected to a unidirectional microphone (Sennheiser ME64) at 48 kHz and 24-bit resolution and saved in uncompressed WAVE format. Air temperature and relative air humidity were taken with a digital thermo-hygrometer to the nearest 0.1 °C. Recordings were analyzed using the software CoolEdit Pro 2.0 (Syntrillium Software Corp.). Frequency information was obtained through Fast Fourier Transformation (FFT, width 1024 points) with Hanning window function. Audiospectrograms were obtained with Blackman window function at 256 bands resolution. Temporal measurements are given in milliseconds (ms) as range, with mean ± standard deviation in parentheses. Sensitive high-pass filtering was applied to remove background

sound outside the prevalent bandwidth of calls. Analysis of calls and terminology in call descriptions follows the recommendations of Köhler et al. (2017), using the note-centered terminological scheme.

Molecular genetics

For studying genetic differentiation and the molecular phylogenetic position of the new *Chimerella* lineage, the data set used by Köhler et al. (2023) was complemented by newly generated sequences from the newly obtained samples, using the same mitochondrial DNA fragments formerly used by these authors. Moreover, we added data for three nuclear gene fragments, as specified below. The data set used to infer a mitochondrial phylogeny also included representative species of other genera currently recognized in the family Centrolenidae. *Allophryne ruthveni*, family Allophrynidae, the sister taxon of Centrolenidae (Guayasamin et al. 2009), was used as the outgroup.

The mitochondrial phylogenetic analysis was based on DNA fragments of the mitochondrial genes for 12S rRNA (12S), 16S rRNA gene (16S; two fragments), NADH-de-

hydrogenase subunit 1 (ND1) and cytochrome b (cob). DNA was extracted from tissue samples using a standard salt protocol and the gene fragments PCR-amplified (and subsequently sequenced with the respective forward primers) with the following primers and PCR protocols: (AAACTGGGATTAGATACCCCACTAT) 12SAL 16SR3 (TTTCATCTTTCCCTTGCGGTAC) of Koch-ER et al. (1989) and HRBEK & LARSON (1999); 94 °C(908), [94 °C(45s), 52 °C(45s), 72 °C(90s) × 33], 72 °C(300s). 16SL3 (AGCAAAGAHYWWACCTCGTACCTTTTG-CAT) and 16SAH (ATGTTTTTGATAAACAGGCG) of Vences et al. (2003); 94 °C(90s), [94 °C(45s), 52 °C(45s), 72 °C(90s) × 33], 72 °C(300s). 16SAr-L (5'-CGCCTGTT-TATCAAAAACAT-3') and 16SBr-H (5'-CCGGTCT-GAACTCAGATCACGT-3') of PALUMBI et al. (1991); 94 °C(90s), [94 °C(45s), 50-53 °C(45 s), 72 °C(90s) × 36-40], 72 °C(300s). Cytb-a (CCATGAGGACAAATAT-CATTYTGRGG) and Cytb-c (CTACTGGTTGTCCTC-CGATTCATGT) of Bossuyt & MILINKOVITCH (2000); 94 °C(90s), [94 °C(30s), 53 °C(45s), 72 °C(90s) × 35], 72 °C(600s). No new sequences were added for ND1 but existing sequences of this gene were added to the analysis to better resolve the deep nodes in the phylogeny.

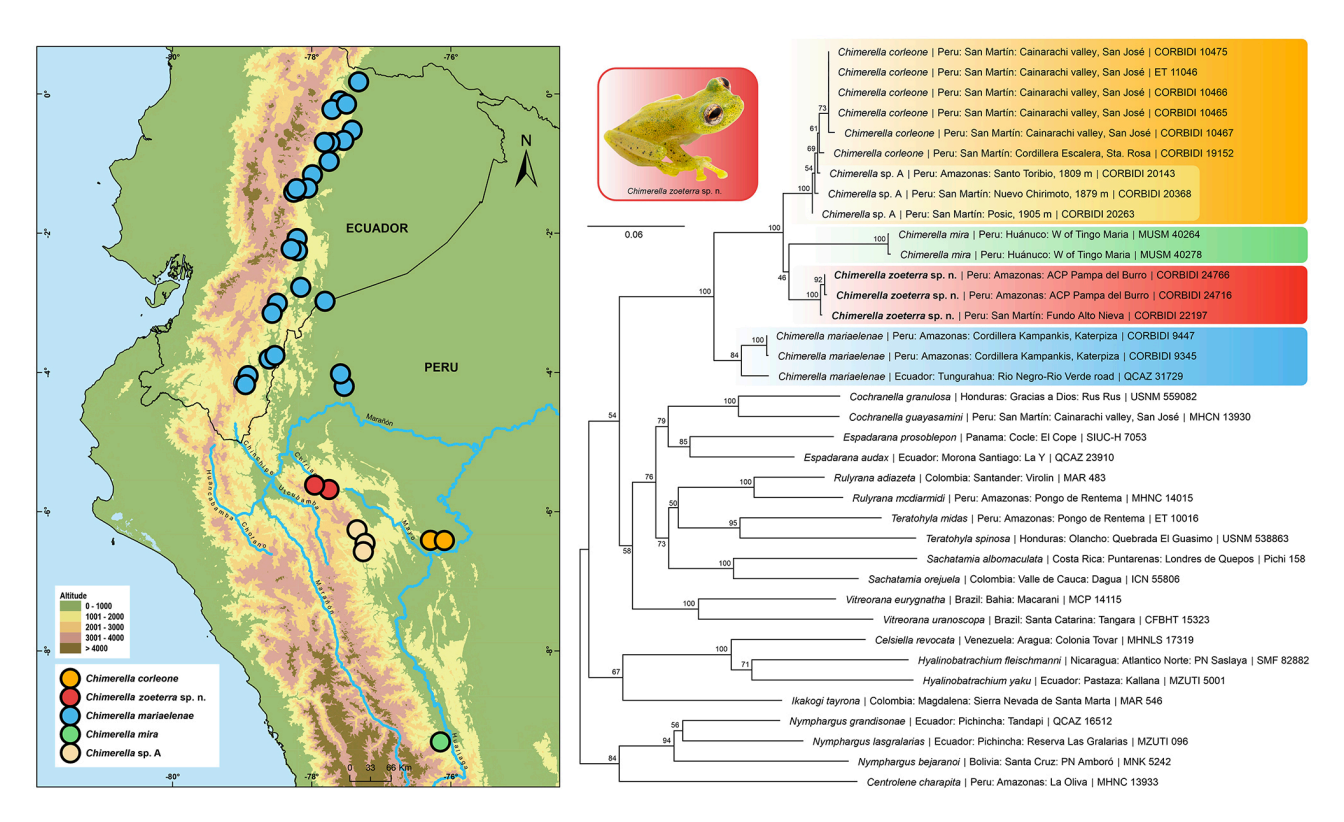


Figure 1. Distribution map and phylogenetic tree of *Chimerella* species. Left: Map of central-western South America showing the known distribution of *Chimerella* species/populations (Guyasamin et al. 2020, Köhler et al. 2023, this study). Colors of dots for the species correspond to those used in the phylogenetic tree on right side. Right: Maximum likelihood phylogenetic tree of centrolenid frogs focusing on *Chimerella* inferred from an alignment of 3634 nucleotides of the mitochondrial genes for 12S and 16S rRNA, ND1, and cytochrome b. *Allophryne ruthveni* was used to root the tree (removed for better graphical presentation). Numbers at nodes are bootstrap values in percent (1000 replicates; not shown for some of the most shallow nodes). Sequences from samples of *C. zoeterra* sp. n. were newly obtained for this study. The taxon name is followed by the sample locality and collection number of the voucher specimen.

To assess variation and divergence in nuclear genes, we sequenced fragments of three single-copy proteincoding nuclear-encoded genes after amplifying them in nested PCR approaches: (i) the recombination-activating gene 1 (RAG-1), first using the primers Rag1-Mart Fl1 (AGCTGGAGYCARTAYCAYAARATG) and Rag-1Mart R6 (GTGTAGAGCCARTGRTGYTT), modified from MARTIN (1999), and then Rag-1AmpF2 (ACNGGNMGI-CARATCTTYCARCC) and Rag-1-UC-R TTGGACTGC-CTGGCATTCAT of CHIARI et al. (2004), with PCR protocol 94 °C(240s), [94 °C(45s), 45 °C(40s), 72 °C(120s) × 45], 72 °C(600s) for both PCR rounds; (ii) a fragment of sacsin (SACS) using external primers SACSF2 (AAYATHAC-NAAYGCNTGYTAYAA) and SACSR2 (GCRAARTGNC-CRTTNACRTGRAA) and internal primers SACSNF2 (TGYTAYAAYGAYTGYCCNTGGAT) and SACSNR2 (CKGTGRGGYTTYTTRTARTTRTG) and with cycling protocol for both PCRs: 94 °C(240s), [94 °C (45s), 45 °C (40s), 72 °C (120s)] × 45, 72 °C (600s) according to Shen et al. (2012); and (iii) a fragment of the KIAA1239 gene, with external primers KIAA1239-F1 (CARCCTTGGGTNT-TYCA), KIAA1239-R1 (CMACAAAYTGGTCRTTR), and internal primers KIAA1239-NF1 (GAGCCNGAYATH-TTYTTYG) and KIAA1239-NR1 (TTCACRAANCCM-CCNG) (SHEN et al. 2012), with the same cycling protocols as those used for SACS. PCR products were purified with Exonuclease I and Shrimp Alkaline Phosphatase digestion, and the purified products along with sequencing primers were shipped to LGC Genomics (Berlin) for sequencing on automated capillary sequencing instruments. Chromatograms were checked for base-calling errors and edited with CodonCode Aligner 6.0.2 (Codon Code Corporation, Dedham, MA, USA). Newly generated sequences were submitted to GenBank (accession numbers: PX403073-PX403075, PX403076-PX403078, and PX410031-PX410049). A table with all samples used, the associated GenBank accession numbers and sequences, as well as voucher number and locality, is available from the Zenodo repository (https://doi.org/10.5281/zenodo.14019863) along with the alignment files.

We analyzed the mitochondrial genes separately from the nuclear-encoded genes, with the goal to assess concordance in the differentiation of nuclear encoded and mitochondrial genes. We used Concatenator (VENCES et al. 2022) to align the five mitochondrial gene fragments with the G-INS-i algorithm of MAFFT (KATOH & STAND-LEY 2013), remove alignment positions with > 95% gaps, and export a concatenated alignment partitioned by gene. The alignment was then submitted to maximum likelihood phylogenetic analysis in IQ-Tree 1.6.12 (NGUYEN et al. 2015), including the inference of the best partition and substitution models with Modelfinder (KALYAANA-MOORTHY et al. 2017) under the MFP+MERGE setting. Node support was tested with 1000 full bootstrap replicates. Based on the Modelfinder results, the analysis was run with a partition of two character subsets: (i) 12S, the two 16S fragments; and (ii) cob and ND1, both with a TIM2+F+I+G4 model.

Table 1. Variation of morphological measurements (in mm) of the type series of *Chimerella zoeterra* sp. n. Mean \pm SD is given in parentheses following the range. See text for abbreviations.

	Females n = 8	Males n = 30
SVL	20.5-22.4 (21.5±0.6)	17.7-20.7 (19.3±0.7)
HL	6.3-7.3 (7.0±0.3)	5.8-7.0 (6.4±0.3)
HW	7.9-8.8 (8.4±0.3)	6.9-8.0 (7.5±0.3)
TD	0.7-1.3 (0.9±0.2)	0.6-1.0 (0.7±0.1)
IND	1.6-2.0 (1.8±0.1)	1.4-1.9 (1.7±0.1)
IOD	2.3-2.7 (2.5±0.2)	2.0-2.7 (2.3±0.2)
ED	2.7-3.0 (2.9±0.1)	2.3-3.1 (2.7±0.2)
EW	1.7-2.1 (1.9±0.1)	1.4-1.9 (1.7±0.2)
END	1.9-2.2 (2.0±0.1)	1.3-2.0 (1.7±0.2)
HaL	6.9-8.0 (7.3±0.4)	5.6-7.2 (6.5±0.3)
TL	11.5-13.1 (12.4±0.5)	10.4-12.1 (11.0±0.4)
THL	11.4-13.2 (12.2±0.7)	10.5-12.0 (11.2±0.4)
FL	9.1-10.6 (9.9±0.5)	8.4-10.0 (9.0±0.4)

The nuclear gene fragments were aligned and trimmed to equal length for each fragment, respectively, in MEGA7 (KUMAR et al. 2016). We then graphically visualized relationships among alleles (haplotypes) of Rag-1 using the Fitchi approach (MATSCHINER 2016) as implemented in Hapsolutely (VENCES et al. 2024b). Alleles (haplotypes) of the nuclear gene were inferred in Hapsolutely using the PHASE algorithm (STEPHENS et al. 2001) and the Fitch tree calculated by maximum parsimony.

Species concept

We use congruence in observed differences in morphological characters, color pattern, traits of the advertisement calls, and the inferred genetic divergences as species delimitation criteria (Padial et al. 2010), following the general lineage or unified species concept (SIMPSON 1951, WILEY 1978, DE QUEIROZ 1998, 2007).

Nomenclatural act

The electronic edition of this article conforms to the requirements of the amended International Code of Zoological Nomenclature, and hence the new name contained herein is available under that Code from the electronic edition of this article. This published work and the nomenclatural act it contains have been registered in ZooBank, the online registration system for the ICZN. The LSID (Life Science Identifier) for this publication is: urn:lsid:zoobank. org:pub: 4E1E98D1-E113-4C67-8F39-oDEAoAC1F383. The electronic edition of this work was published in a journal with an ISSN, and has been archived and is available from the following digital repositories: zenodo.org, salamandrajournal.com.

Results Phylogenetic relationships

The maximum likelihood tree (Fig. 1) inferred from a 3634 bp alignment of the mitochondrial 12S, 16S, ND1, and cob genes largely agreed with a previous reconstruction (KÖHLER et al. 2023) in placing all Chimerella samples in a highly supported monophyletic group (bootstrap support [BS] 100%), and samples of each species also formed highly supported groups (BS 84-100%). Basal nodes of the centrolenid phylogeny were not reliably resolved and did not fully agree with current higher-level classification, but these topological aspects also had low bootstrap support (BS 24–58% for the three most basal nodes; Fig. 1). Samples of Chimerella sp. A from Santo Toribio, Nuevo Chirimoto, and Posic were very closely related to C. corleone, without an appreciable amount of differentiation according to the branch lengths of the tree (see KÖHLER et al. 2023 for a discussion of these morphologically divergent populations). The focal lineage from Fundo Alto Nieva and Pampa del Burro was placed sister to C. mira, but no significant support for the respective node was found by bootstrap analysis (BS 46%). Thus, the sister relationships of C. mira and the focal lineage is barely supported with the data at hand. However, the data provide clear evidence that the focal lineage is not nested within one of the recognized nominal species of Chimerella.

The focal lineage had uncorrected p-distances in the 16S rRNA gene (for a fragment of 475 nucleotides at the 3' terminus of the gene without missing data in any sequence) of 2.3–2.7% compared to *C. corleone*, 3.0–3.2% to *C. mariaelenae*, and 3.8–4.2% to *C. mira*. Except for the distance to *C. mira*, these distances are at slightly lower levels as between the three nominal species of *Chimerella* (3.5–4.0%), but are at equal level as those found between numerous closely related species within other centrolenid genera (as explored by Köhler et al. 2023).

The haplotype networks of the three nuclear genes analyzed here (Fig. 2) did not detect any haplotype sharing between the main lineages identified by the mitochondrial

data. Due to poor DNA quality, PCRs for several samples and genes failed despite multiple repeated attempts, and therefore only the RAG-1 network contains all lineages; the SACS and KIAA1239 networks lack sequences of *C. corleone*, and the SACS network furthermore lacks *C. mariaelenae* (see Fig. 2). These two additional genes, however, confirm an absence of haplotype sharing between the focal lineage and *C. mira* and *C.* sp. A (which in the mitochondrial tree is very close to *C. corleone*; see Fig. 1); furthermore, the KIAA1239 network also confirms haplotype distinctness of *C. mariaelenae* based on multiple individuals.

Bioacoustics

Our bioacoustic analysis of advertisement calls of the focal lineage of Chimerella from Pampa del Burro revealed qualitative and quantitative differences when compared to nominal congeners (see detailed call description below). Calls of C. mira agree with those of the focal lineage in having pulsatile notes qualifying as 'Trii' calls as defined by Duarte-Marín et al. (2022). However, note duration in calls of *C. mira* is significantly longer, compared to calls of the focal lineage (42–85 vs. 26–35 ms) and inter-note intervals within calls are shorter (160-239 vs. 265-432 ms). Calls of C. mariaelenae differ from those of the focal lineage by much shorter note duration (3-7 vs. 26-35 ms), higher dominant frequency (6460-7752 vs. 5648-6058 Hz) and simple, unpulsed 'Tic' calls (sensu Duarte-Marín et al. 2022). Calls of C. corleone equally qualify as 'Tic' calls and furthermore differ by shorter note duration from calls of the focal lineage (10-15 vs. 26-35 ms). For more detailed call comparisons, see sections below and Table 2. Our bioacoustic findings strongly indicate respective lineage divergence, as the differences observed are clearly beyond those to be expected from intraspecific call variation (see Köhler et al. 2017). This is particularly true for centrolenid species, where evolutionary divergent lineages may emit rather similar calls (e.g., GUAYASAMIN et al. 2020, KÖHLER et al. 2023).

Table 2. Comparative parameters and characters of advertisement calls of *Chimerella* species. EC = Ecuador, PE = Peru.

	Notes/ call	Note duration [ms]	Dominant frequency [Hz]	Pulsatile notes	Number of males/ calls analyzed
Chimerella corleone PE: San José	2	10-15	6485-6526	no	1/1
Chimerella mariaelenae PE: Cord. Kampankis	2	3-7 (5.4±1.4)	6706-7633 (7182±292)	no	4/12
Chimerella mariaelenae EC: Pangayaku Creek	2-10	4-7 (6.0±0.9)	6460-7752 (7222±387)	no	2/7
Chimerella mira PE: W of Tingo Maria	2-3	42-85 (64.6±11.7)	5543-6135 (5897±148)	yes	4/12
<i>Chimerella zoeterra</i> sp. n. PE: Pampa del Burro	3-5	26-35 (29.8±2.8)	5648-6058 (5938±309)	yes	2/4

Morphology

Our morphological examination and comparison of *Chimerella* individuals showed specimens of the focal lineage to mainly differ in color pattern in life from *C. corleone* and *C. mira* with respect to dorsal and iris coloration (see below). However, the focal populations are morphologically indistinguishable from *C. mariaelenae* in life. Although some populations of *C. mariaelenae* may differ slightly from the focal populations by details of the iris col-

oration, these color differences are not diagnostic when considering overall intraspecific variation of this character in *C. mariaelenae*. We observed, however, differences in dorsal coloration between equally preserved specimens of *C. mariaelenae* and the focal lineage, with *C. mariaelenae* specimens exhibiting a distinctly lavender color, whereas specimens of the focal lineage exhibit a faint lavender hue only. Morphometric data are summarized in Table 1, while qualitative morphological characters are illustrated in Figures 3–5 and 7.

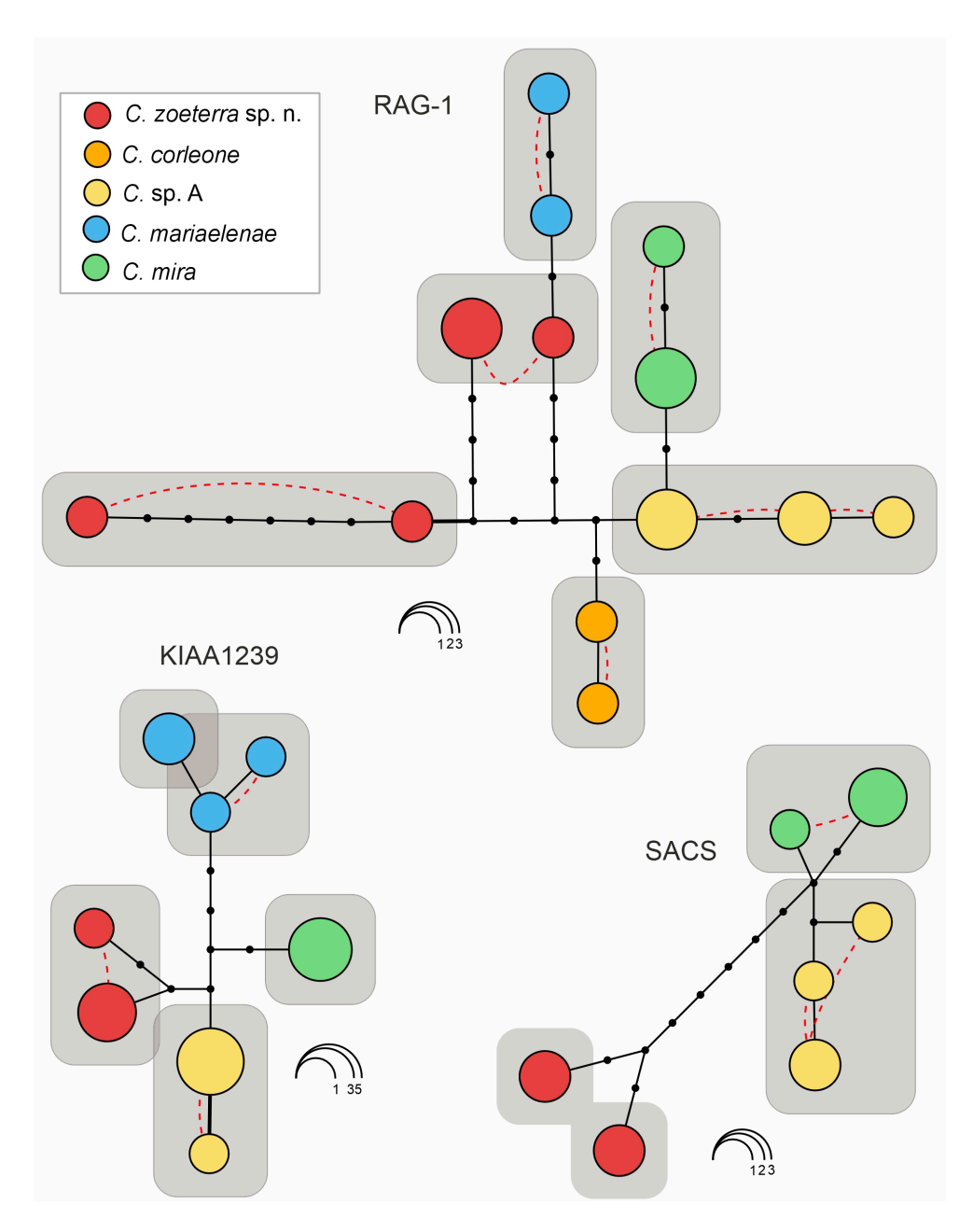


Figure 2. Haplotype networks (Fitch tree genealogies) of the three nuclear-encoded protein-coding genes RAG-1 (1019 bp; 10 specimens), SACS (1032 bp; 6 specimens), and KIAA1239 (872 bp; 9 specimens). Note that the networks were reconstructed from phased sequences and each specimen is represented by two sequences. Stippled red lines indicate instances of co-occurrence of different alleles in the same individual.

Taxonomy

Our results from molecular genetics, namely reciprocal monophyly, substantial mitochondrial distances, and lack of haplotype sharing with other *Chimerella* species in nuclear-encoded genes, as well as the bioacoustic differentiation of the focal lineage from known species of *Chimerella*, provide independent lines of evidence for the presence of a distinct evolutionary lineage at the species level. We in the following describe the populations from white sand outcrops in Yungas montane forests of Amazonas and San Martín departments as a species new to science.

Chimerella zoeterra sp. n. Figs 3-5, 7A-B

ZooBank LSID: urn:lsid:zoobank.org:act: 4F43CEF9-4536-408E-84B4-28EF22C38E6D

Holotype: CORBIDI 24684, an adult male, from El Arenal in the Área de Conservación Privada Pampa del Burro (-5.618962°, -77.947475°, 1770 m a.s.l.), Yambrasbamba district, Bongará province, Amazonas department, Peru, collected on 5 March 2023 by P. J. VENEGAS, L. A. GARCIA-AYACHI, S. BULLARD, E. QUISPE, and J. D. VALENCIA.

Paratypes (38): CORBIDI 24677, 24685–86, 24688, 24691, 24706, 24715, 24717–24720, 24756, and 24770, adult males, CORBIDI 24678, 24716, 24762, and 24766, adult females, same data as holotype; CORBIDI 22152–22153, 22155–22157, 22159, 22162, 22165–22168, 22170, 22172, 22177, and 22179, adult males, CORBIDI 22164, 22173, 22178, and 22180, adult females, CORBIDI 22160, an unsexed juvenile, from Fundo Alto Nieva (-5.676331°, -77.761172°, 1982 m a.s.l.), Pardo Miguel district, Rioja province, San Martín department, Peru, collected on 21 January 2020 by L. A. GARCIA-AYACHI and J. ORMEÑO.

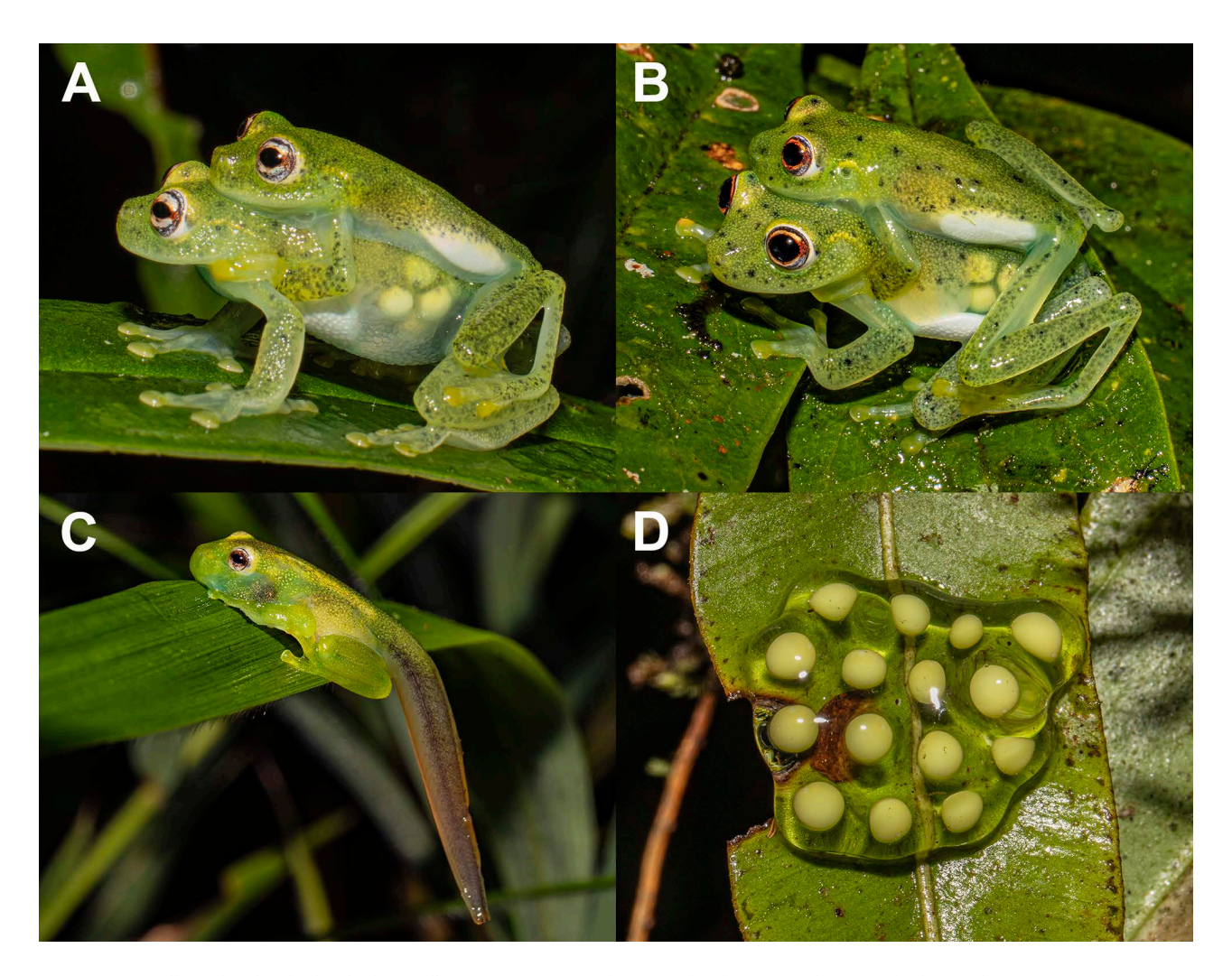


Figure 3. Uncollected individuals of *Chimerella zoeterra* sp. n. and an egg clutch in situ, photographed at night on 22 January 2020 at Fundo Alto Nieva, Amazonas department, Peru: (A, B) amplectant couples; (C) a metamorph at Gosner stage 44 at ca. 20 cm height on a leaf; and (D) an egg clutch containing fifteen eggs. Photographs by L. A. GARCÍA-AYACHI.

Definition: A species in the genus Chimerella, based on molecular relationships and shared morphological traits, characterized by the following combination of characters: (1) dentigerous processes of vomer and vomerine teeth absent; (2) snout truncate in dorsal view, truncate or nearly truncate in lateral profile; canthus rostralis curved in dorsal view, rounded in cross-section; nostrils not protuberant; (3) tympanum and tympanic annulus evident, round, its diameter about 27% of eye diameter; supratympanic fold well defined, concealing the upper edge of tympanum; (4) dorsal skin finely granular, lacking enlarged tubercles; skin on venter and ventral surfaces of thighs areolate; (5) a pair of enlarged subcloacal warts; (6) ventral parietal peritoneum transparent (condition P0 sensu CISNEROS-HE-REDIA & McDiarmid 2007); iridophores covering pericardium, liver, gallbladder, visceral peritonea, and testes; kidneys and urinary bladder lacking iridophores (condition V₅); (7) liver with two broadly rounded right/left lobes (condition H2); (8) humeral spine and single subgular vocal sac present in adult males; (9) webbing absent or ba-

sal between inner fingers, moderate between outer fingers; webbing formula: $III(2\frac{1}{2}-2\frac{1}{3}) - (2^{+}-2\frac{1}{2})IV$; (10) webbing extensive between toes; webbing formula I2 - (2-2+)II1 - $(2\frac{1}{2}-3^{-})III(1-1\frac{1}{2}) - (2^{-}-3)IV(2^{-}-3^{-}) - (1-1^{+})V;$ (11) enamelled fringe absent on postaxial edge of finger IV; ulnar fold ill-defined; tarsal fold absent; enlarged tubercles on ventrolateral edges of arm and tarsus absent; (12) prepollical spine not protruding externally; unpigmented nuptial pad present (Type I); (13) finger I slightly longer than finger II; (14) diameter of eye three times wider than width of disc on finger III; (15) in life, dorsum pale green bearing scattered dark gray or black dots at night (Fig. 3A-B), and light yellow-green covered by a dark green punctuation and scattered black dots during the day (Fig. 4); venter transparent; bones green (Fig. 4B, G); (16) in preservative, dorsal surface vellowish cream covered by lavender minute flecks and few scattered black dots (Fig. 5A; limbs flecked with melanophores; ventral surfaces cream (Fig. 5B); (17) in life, iris creamy white bearing dark gray reticulations and a thin orange-red median streak (Fig. 4H) or only gray flecks

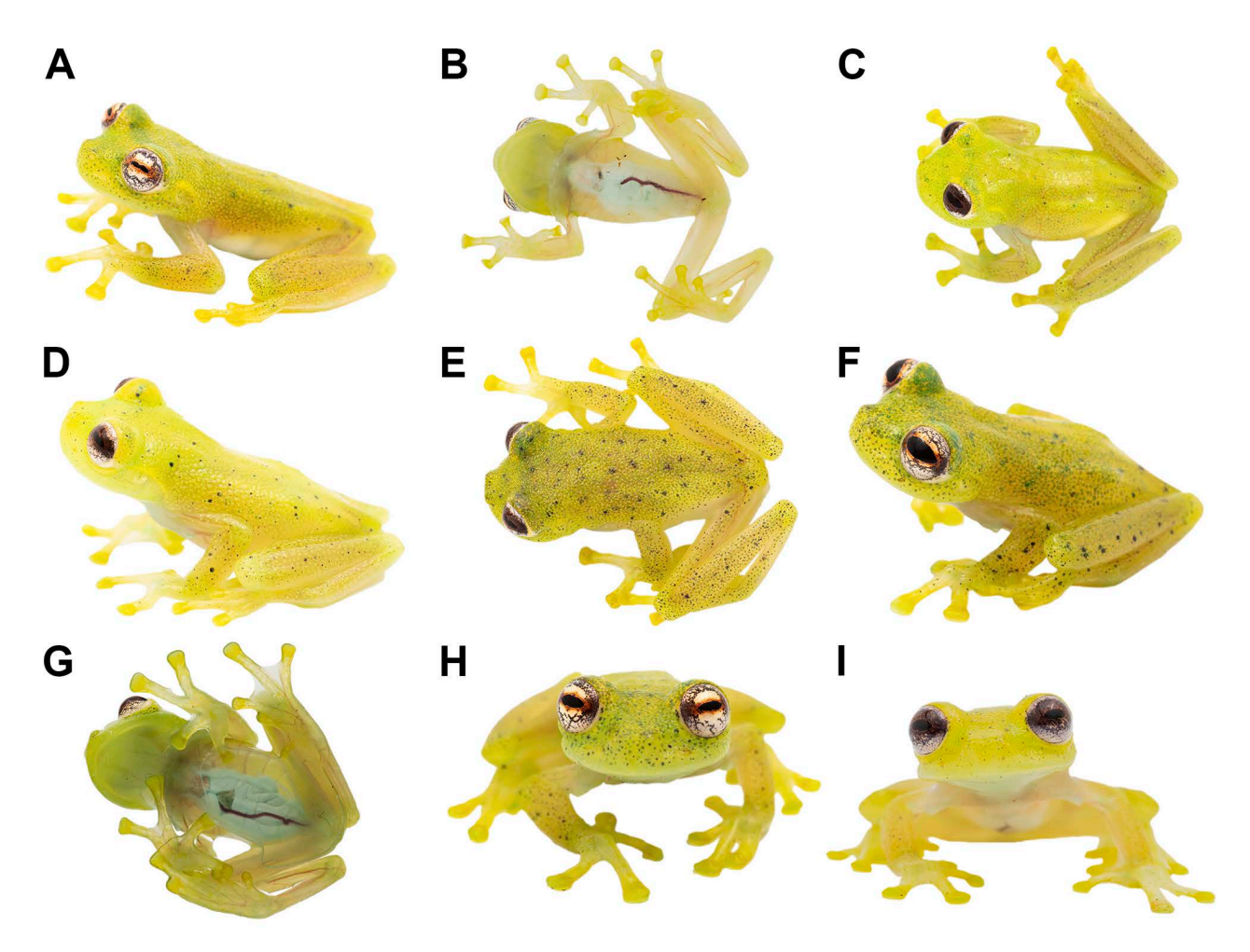


Figure 4. Adult male specimens of *Chimerella zoeterra* sp. n. in life: (A) dorsolateral and (B) ventral views of male holotype CORBIDI 24684; (C) dorsal view of CORBIDI 24688; (D) dorsolateral view of CORBIDI 24717; (E) dorsal view of CORBIDI 24677; (F) dorsolateral and (G) ventral views of CORBIDI 24685; (H) and (I) frontal views of CORBIDI 24691 and 24715, respectively. Photographs by E. Quispe.

and a bold reddish gray median streak (Fig. 4J); circumpupillary ring absent; (18) dorsal surfaces of fingers and toes lacking melanophores, except for toes IV and V; (19) males call from the upper surface of leaves; calls consist of 3–5 pulsatile notes, each with a duration of 26–35 ms, with inter-note intervals within calls of 265–432 ms, and dominant frequency of 5648–6058 Hz; (20) fighting behavior unknown; (21) egg clutches observed on the surface of fern leaves along riparian vegetation; one of these clutches had 15 cream eggs and were deposited in a viscous translucent jelly; (22) tadpoles in early developmental stages unknown (see below); (23) minute body size (sensu Guayasamin et al. 2020), SVL in adult males 17.7–20.7 mm (n = 30); SVL in adult females 20.5–22.4 mm (n = 8).

Diagnosis: *Chimerella zoeterra* can be easily distinguished from *C. corleone* and *C. mira* by having a light yellow-green

dorsum covered by a dark green punctuation and scattered black flecks, whereas the dorsum is yellow-green with scattered vellow flecks in C. mira and C. corleone. Moreover, although the irises of the three species are silvery or creamy white, each species possesses a different pattern: bearing a conspicuous dark gray spotting, reticulations, and an orange or red median streak in C. zoeterra; black fine spotting with a median brown streak in C. mira; and black fine reticulations with a median brown streak in C. corleone. Chimerella zoeterra is morphologically very similar to C. mariaelenae (Fig. 6). In life, only some individuals of C. mariaelenae can be distinguished from C. zoeterra by having a dark gray or blue ring outlining the iris without peripheral reticulations (Fig. 6C), while all specimens of C. zoeterra (n = 39) possess an orange or orange-red medial streak bearing peripheral gray reticulations. In preserved specimens (ethanol 70%), C. zoeterra is cream with a lav-

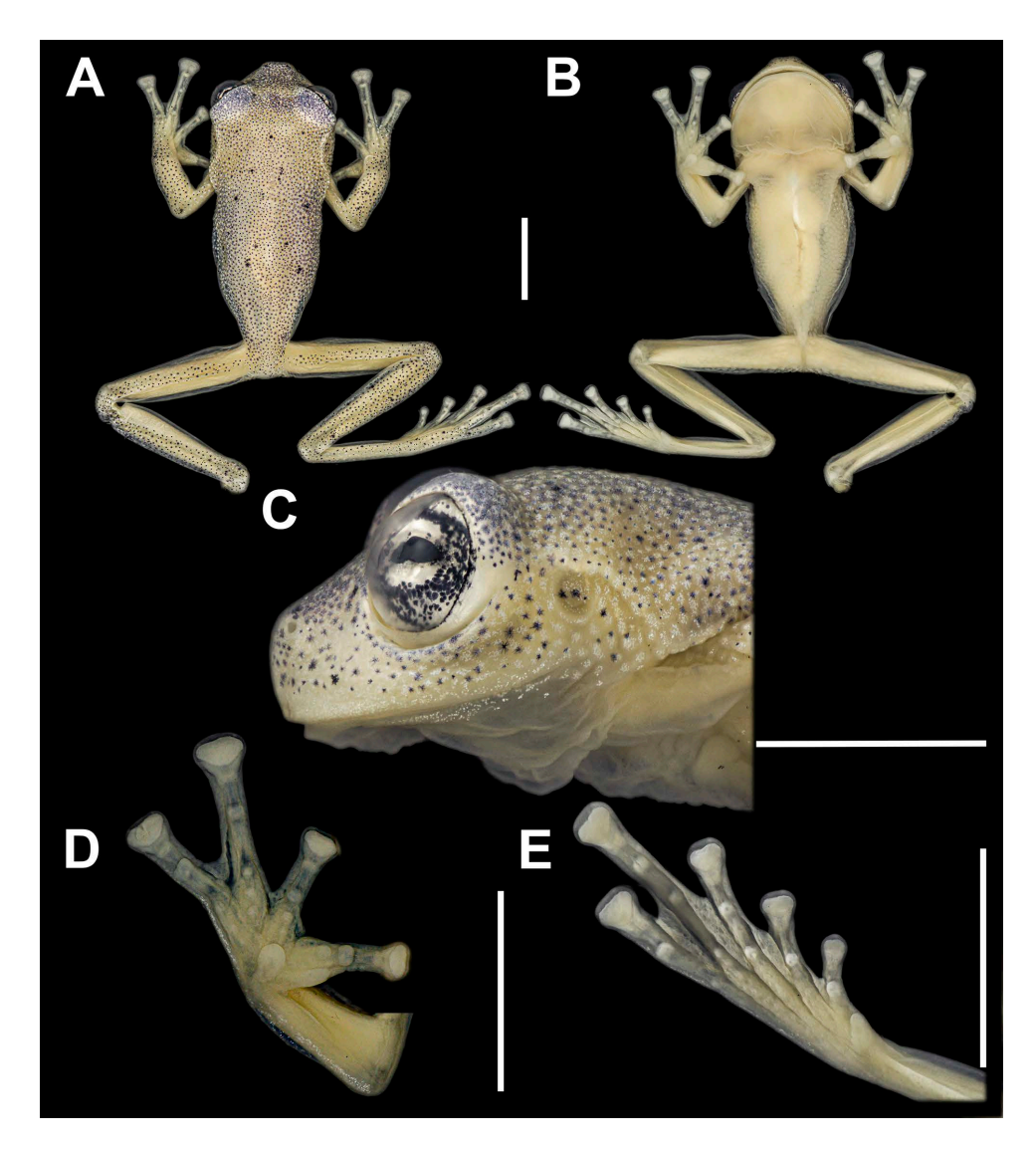


Figure 5. Preserved male holotype of *Chimerella zoeterra* sp. n. (CORBIDI 24684) in (A) dorsal, and (B) ventral views of entire body; (C) head in lateral profile; (D) right palm; and (E) right sole. Scale bars = 10 mm. Photographs by L. A. GARCÍA-AYACHI.

ender hue (Fig. 7A, B) vs. distinctly lavender in *C. mariaelenae* (Fig. 7C, D). However, the advertisement call of *C. zoeterra* mainly differs from that of *C. mariaelenae* by being composed of pulsed notes (vs. unpulsed notes) and notes of longer duration (26–35 vs. 3–7 ms).

Description of the holotype: Adult male, SVL 19.4 mm, in good state of preservation with the left foot removed and preserved as a tissue sample for molecular analyses (Fig. 5). HW slightly wider than body; HW 37% of SVL; HW 1.07 times HL. Snout truncate in dorsal view, nearly truncate in lateral profile; END/ED 0.63; END/IOD 0.71. Loreal region concave, nostrils not protuberant, round; internarial region barely concave anterodorsally; canthus rostralis illdefined, curved in dorsal view, rounded in cross-section. Eyes directed anterolaterally, angled ~ 45° relative to midline of body; ED 2.3 times wider than width of disc on finger III; ED 41% of HL and 111% of IOD. Tympanum noticeable with tympanic annulus visible, more evident ventrally than dorsally, annulus and membrane colored as dorsum; supratympanic fold well-defined obscuring the dorsal edge of tympanum, tympanum round with slight dorsal inclination. Dentigerous processes on vomers absent; choanae large, circular, separated more widely than nostrils; tongue wider than long, notched posteriorly, covering most of floor of mouth, posterior quarter free; vocal slits present, wide, oblique, and lateral to the tongue. Forelimbs robust, with forearm flattened and roughly 1.4 times as wide as arm; ulnar fold present, ill-defined, white; tubercles on ventrolateral edge of arm absent; humeral spine externally visible as an elongated bump, slightly less defined in preservative than in life. Relative length of fingers: II < I < IV < III; finger discs distinctly expanded, those on fingers I, II, and IV truncate, on fingers III gently rounded, larger than toe discs; width of disc on finger III 53.7% of ED; webbing absent between fingers I and II, basal webbing between fingers II and III, and moderate between III and IV, webbing formula III2½-2+IV. Prepollex concealed; subarticular tubercles round, distinct; supernumerary tubercles present, palmar tubercle round and small, thenar tubercle distinct, ovoid, elongate; nuptial pads present, medium-size, nuptial excrescences visible on dorsal and ventrolateral sides (Type I sensu Guayasamın et al. 2020). Hind limbs slender, TL 53% of SVL; tarsal fold absent; tubercles on ventrolateral edge of tarsus absent. Relative length of toes: I < II < III < V < IV; toe discs expanded, round; inner metatarsal tubercle narrow, elongated, ovoid, low; outer metatarsal tubercle absent. Webbing formula of feet: I2⁻-2⁺II1-2½III1½-3⁻IV2½-1⁺V. Dorsal skin finely granular; skin on venter and ventral sides of thighs areolate, skin on throat smooth; cloacal opening at level of upper thighs, concealed by distinct superior dermal fold; cloacal region coarsely areolate; a pair of enlarged subcloacal warts present, ill-defined; crenulated flaps absent.

Measurements (in mm): SVL 19.4, HL 6.8, HW 7.3, TD 1.03, IND 1.3, IOD 2.5, ED 2.8, EW 1.4, END 1.8, HaL 6.4, TL 10.4, THL 10.5, FL 8.6.

In life (Fig. 4A–B), dorsal surface light yellow-green covered by green punctuations and bearing scattered black dots and a faint green interorbital bar. Ventrolateral region

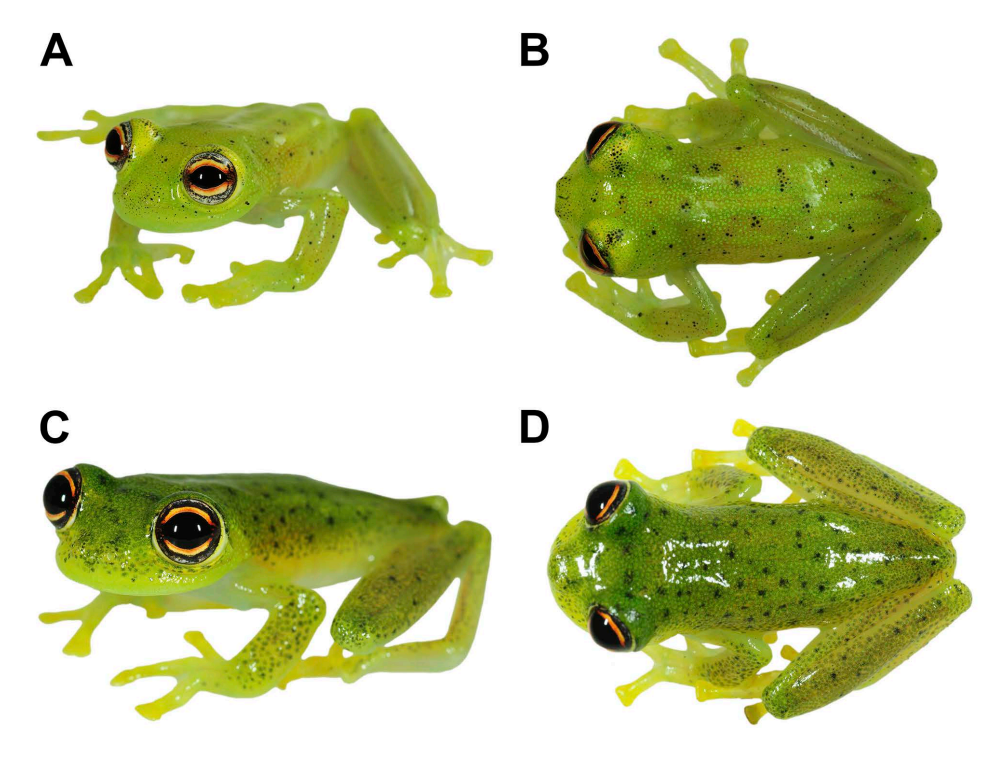


Figure 6. Frontolateral and dorsal views of two adult males of *Chimerella mariaelenae* from the Cordillera de Kampankis, Peru, in life: (A, B) CORBIDI 9453 and (C, D) CORBIDI 9472. Photographs by A. CATENAZZI.

creamy white. Ventrally, throat and chest are pale green, limbs and belly are pale sulfur yellow, and digital discs yellow. Clear ventral parietal peritoneum showing white heart (covered by a white pericardium), white digestive tract, liver, and testes; gallbladder dirty white; clear peritoneum covering the urinary bladder; bones pale yellow-green and sclerotic ring white. Iris creamy white bearing dark gray reticulation and flecks, and with an orange-red median streak.

After 28 months in 70% ethanol (Fig. 5), dorsal surface cream covered by a lavender punctuation bearing scattered black flecks, the lavender punctuation is denser on eyelids and the interorbital region (forming a faint lavender interorbital bar), and less dense on limbs and feet. Ventral surface cream. Heart, liver, and intestine slightly visible through the belly skin.

Variation: Sexual dimorphism is noticeable in size (mean SVL 19.3 mm in males vs. 21.5 mm in females), and males possess vocal slits and humeral spines. For the variation in size and proportions see Table 1. The density of black dots and green punctuation varies between individuals from few scattered black dots and inconspicuous green punctuation (Fig. 4C–D) to densely scattered black dots and conspicuous green punctuation (Fig. 4F–G). The specimen CORBIDI 24685 has the heart and the gallbladder covered by a thin layer of iridophores that give it a coppery coloration (Fig. 4G). However, the most noticeable interspecific variation in *Chimerella zoeterra* is in the iris coloration, particularly color and width of the medial streak, as well as the presence or absence of dark gray reticulations in the periphery of the iris. In most individuals, a thin or-

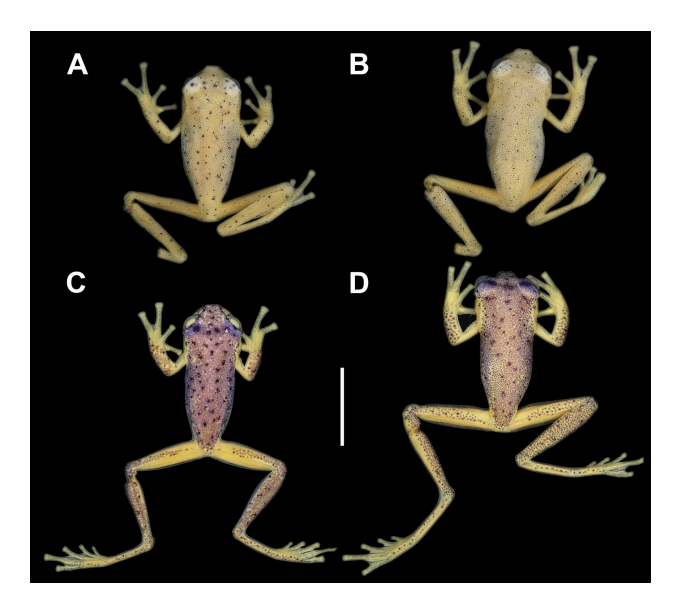


Figure 7. Comparison of dorsal color pattern of preserved specimens of *Chimerella zoeterra* sp. n.: (A) adult male CORBIDI 22152, (B) adult female CORBIDI 22173; and *C. mariaelenae*: (C) adult male CORBIDI 11375, (D) adult female CORBIDI 9474. Scale bar = 10 mm. Photographs by L. A. GARCÍA-AYACHI.

ange or orange-red medial streak with gray flecks and reticulations (Fig. 4I) is present, whereas in some individuals a bold dark grayish brown medial streak (Fig. 4J) with or without gray peripheral reticulations is evident (e.g., CORBIDI 24688, 24715, 24717, and 24719). A non-collected metamorph (Gosner stage 44) (Gosner 1960) was observed in situ at night (Fig. 3C). This individual possessed a light green dorsal surface, grayish green tail, and the iris creamy white, bearing a brownish orange median streak.

Distribution and natural history: Chimerella zoeterra is only known from two localities, Pampa del Burro in the upper basin of the Chiriaco River, at elevations of 1770 and 1827 m a.s.l., and Fundo Alto Nieva in the upper basin of the Mayo River, at elevations between 1937 and 1982 m a.s.l., in the departments of Amazonas and San Martín, respectively, northeastern Peru (Fig. 1). At both localities this species inhabits riparian vegetation of black water streams dissecting humid montane forest on white sand outcrops (Fig. 8A-C). The general habitat of C. zoeterra is characterized by humid montane forest with a low canopy with tree heights between 1.5 and 5 m, and abundant epiphytes, such as bromeliads, orchids, ferns, mosses, and lichens (Fig. 8D). All individuals were observed at night during the rainy season (January and March) on leaves of the riparian vegetation, especially ferns, at perch heights between 1 to 2 m. During January, male individuals were actively calling while sitting on top of leaves and several amplectant couples (Fig. 3A-B) and egg clutches on the surface of leaves (Fig. 3D) were observed on riparian vegetation. A metamorph at Gosner stage 44 (Gosner 1960) was photographed perching at 20 cm height on a leaf (Fig. 3C). In March, males were calling only sporadically during short rains and no amplectant couples or egg clutches were observed. According to the Peruvian ecoregions (CDC-UNALM 2006), both known localities of C. zoeterra are located in the Peruvian Yungas ecoregion. Sympatric anuran species observed with *C. zoeterra* were Callimedusa duellmani, Dendropsophus aperomeus, Hyloscirtus phyllognathus, Nymphargus posadae, Pristimantis nephophilus, and Pristimantis sp.

Vocalization: The advertisement calls recorded on 6 March 2023 (03:53 h; air temperature 15 °C) at Pampa del Burro, 1800 m a.s.l., Yambrasbamba district, Bongara province, Amazonas department, Peru, were emitted sporadically and consist of 3 to 5 high-pitched, pulsed notes of short duration (Fig. 9). Notes exhibit considerable amplitude modulation, with maximum call energy present at the beginning of the note, continuously decreasing towards its end. Pulse structure is irregular within notes, with pulses being partly fused. Consequently, the total number of pulses per note is not reliably countable, but in several cases 3 to 5 separated pulses are evident within notes. Pulse rate within notes ranges approximately around 240 pulses/second. The character of the notes would qualify as a 'Trii' call according to the definition of DUARTE-MARÍN et al. (2022). Within calls, inter-note intervals slightly increase in duration from the beginning towards the last note. The initial note of each call exhibits a slightly lower relative amplitude when compared to consecutive notes of the same call. Numerical parameters of 4 analyzed calls from two individuals are as follows: number of notes per call 3–5 (4.0 \pm 0.8); call duration 771–1501 ms (1100.0 \pm 303.1 ms); note duration 26–35 ms (29.8 \pm 2.8 ms); inter-note interval within calls 265–432 ms (320.9 \pm 47.0 ms); note repetition rate within calls ranges between 2.2–3.5 notes/second; dominant frequency 5648–6058 Hz (5938 \pm 309 Hz); prevalent bandwidth 3800–7800 Hz, with a weak second peak at around 12 kHz.

Comparative call data: Regular advertisement calls of *C. mariaelenae* recorded on August 2011 (air temperature 17.6 °C) in the Cordillera de Kampankis (1100 m a.s.l.), Amazonas department, Peru, analyzed for comparison, usually consist of two high-pitched, simple notes of very short duration (Fig. 9), qualifying as 'Tic' calls sensu DUARTE-MARÍN et al. (2022). In a few cases, single notes were

emitted in isolation. Notes exhibit some moderate amplitude modulation, with maximum call energy being present at the beginning of the note, rapidly decreasing towards its end. Virtually, in the oscillogram, some notes seem to contain a second pulse of low call energy, but we allocate this phenomenon to slight echo effects present in the recording (therefore virtual secondary pulses were not considered to be part of the note). Numerical parameters of 12 analyzed calls of four individuals are as follows: number of notes per call 2; call duration 357–402 ms (394.3 \pm 27.1 ms); note duration 3–7 ms (5.4 \pm 1.4 ms); inter-note interval within calls 356–390 ms (367.2 \pm 11.0 ms); dominant frequency 6706–7633 Hz (7182 \pm 292 Hz); prevalent bandwidth 5800–8500 Hz.

Calls of *C. mariaelenae* from Pangayaku Creek (929 m a.s.l.), Napo province, Ecuador, reported by Guayasamin et al. (2020), agree with the calls from Cordillera de Kampankis in note structure, note duration and dominant frequency (Fig. 9). However, these Ecuadorian calls consist of 2–10 notes, although Guayasamin et al. (2020) mentioned



Figure 8. Habitat of *Chimerella zoeterra* sp. n. at Pampa de Burro, Amazonas department, Peru: (A) a black water stream and (B) its white sand bed; (C) montane forest vegetation on white sand outcrops; and (D) the floor of montane forest on white sand outcrops covered by a carpet of epiphytes, such as bromeliads, orchids, ferns, and lichens. Photographs A and C by E. Quispe, B and D by P. J. Venegas.

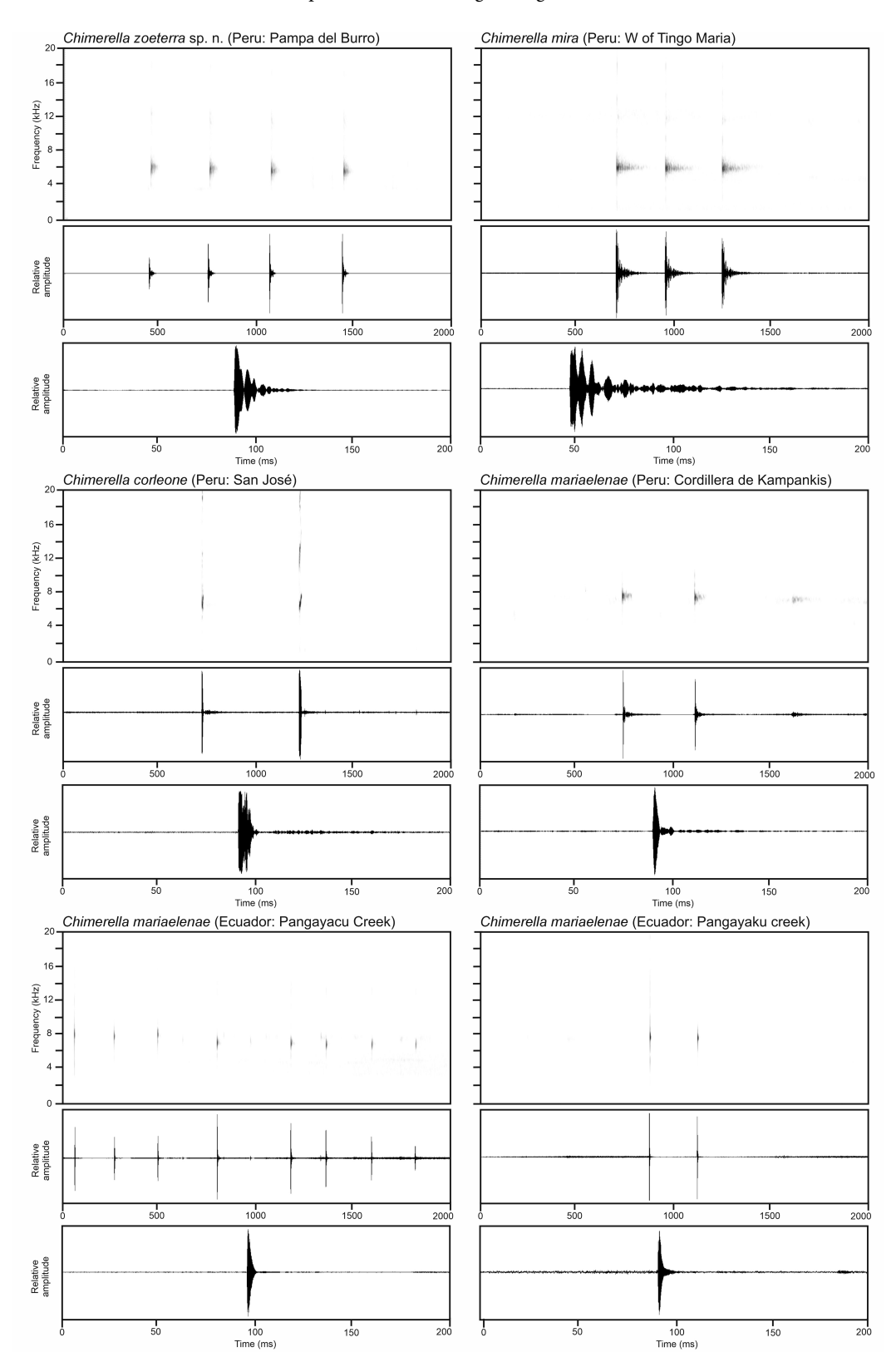


Figure 9. Comparative audiospectrograms and oscillograms of advertisement calls of *Chimerella zoeterra* sp. n., *C. mira*, *C. corleone*, and *C. mariaelenae* at the same temporal (2000 ms) and spectral (20 kHz) scale. Oscillograms at the bottom each show a single note at 200 ms time scale. For Ecuadorian *C. mariaelenae* (bottom row), a call with eight notes is shown (left), as well as a more common two-note call (right). Selective high-pass filtering was applied to the recordings to remove background noise outside the prevalent bandwidths of calls.

that typical calls consist of two notes. Within calls, notes are repeated at shorter intervals (154–262 ms; 202.6 ± 33.9 ms) when compared to the Peruvian calls described above. These differences might easily be explainable with calling motivation or a different social context (see Köhler et al. 2017), and there is little doubt that bioacoustic data support the conspecificity of both reported populations. The somewhat questionable description of *C. mariaelenae* calls by Batallas & Brito (2016) has already been discussed by Köhler et al. (2023).

Advertisement calls of *C. mira* recorded at its type locality in Huánuco department, Peru, consist of 2-3 highpitched, distinctly pulsed notes (Fig. 9) with a comparatively longer note duration of 42-85 ms and a dominant frequency of 5543-6135 Hz (KÖHLER et al. 2023).

Calls of *C. corleone* contain two short notes of simple structure, qualifying as 'Tic' calls sensu Duarte-Marín et al. (2022). Call duration is 521 ms, note duration 10–15 ms; inter-note interval 493 ms, and dominant frequency 6485–6526 Hz (Twomey et al. 2014, Köhler et al. 2023). Comparative call characters of available *Chimerella* calls are provided in Table 2.

Etymology: The specific name *zoeterra* is a noun in apposition and honors ZoeTerra Holdings. The dedication of this species to ZoeTerra is in recognition of its commitment to biodiversity, supporting our herpetological research and conservation work through the non-profit organization Rainforest Partnership, based in Austin, Texas (USA).

Discussion

With the description of *Chimerella zoeterra*, we added a fourth species to the genus *Chimerella*. The total number of centrolenid species known from Peru increased to 39, with Peru being on rank three with respect to the documented number of glassfrog species, after Colombia (74 species) and Ecuador (69 species) (Frost 2025). Given the vast areas of poorly surveyed habitats in Peru, we expect future research to discover numerous additional populations of glassfrogs, many of which probably represent new species-level lineages (see also Twomey et al. 2014, Köhler et al. 2023).

Although very similar in morphology to *Chimerella mariaelenae*, the species status of *C. zoeterra* is evidenced by qualitative and quantitative differences between respective advertisement calls, substantial differentiation in mitochondrial genes, and the lack of haplotype sharing in nuclear genes among the few available samples studied. The two species exhibit an allopatric distribution pattern, with ranges separated by the Marañón River, a major tributary of the Amazon River (Fig. 1). The Marañón River Valley is well-known as a barrier for the distribution of species and a limit of bioregions, separating the Central and the Northern Andes (Cadle 1991, 2001, Winger & Bates 2015, Hazzi et al. 2018, Venegas et al. 2024). Apparently, the range of *C. mariaelenae* along the Amazonian Andean slopes of

Ecuador and northern Peru is disrupted to the south by the Marañón River, as phylogenetically reflected by its sister clade (i.e., *C. zoeterra*, *C. corleone*, and *C. mira*), distributed south of this river. However, the effects of the Marañón River as a barrier for amphibians are still poorly understood due to the lack of herpetological surveys in the Peruvian areas of the Cordillera del Condor above 1100 m elevation (Twomey et al. 2014), and future studies of respective amphibian communities in the Cordillera del Condor and the Cordillera de Colán are needed to get a better understanding of the biogeographical patterns.

Furthermore, our recent field studies indicate that many centrolenids from the Peruvian Yungas ecoregion occur within highly threatened habitats that may vanish quickly and thus demand respective research and immediate conservation action. Otherwise, numerous glassfrog species might be lost prior to their scientific discovery.

Acknowledgements

Specimens were collected under permits RDG No 067-2019-MI-NAGRI-SERFOR-DGGSPFFS and RDG Nº 010-2021-MIDAG-RI-SERFOR-DGGSPFFS granted by the Servicio Nacional Forestal y de Fauna Silvestre (SERFOR). Our fieldwork would not have been possible without the logistic support of EDILBERTO VASQUEZ CORONEL, EDIL GONZALES CARRASCO, and MARIO GARCIA BUSTAMANTE from Perla del Imaza, and CARLOS CALLE and WILMER MONTENEGRO from Fundo Alto Nieva. Moreover, we are grateful to our field assistant Juan D. Valencia and Jesús Ormeño. We are also grateful to Lea Flechtner, Jakob HORZ, and LAILA-DENISE ROTHE for assistance with laboratory work and sequence analysis. We thank JESSE DELIA, JUAN M. GUAYASAMIN, ITALO TAPIA, and EVAN TWOMEY for providing call recordings of C. corleone and C. mariaelenae for comparisons. ALESSANDRO CATENAZZI and EDUARDO QUISPE kindly provided photographs. Santiago Castroviejo-Fisher and an anonymous reviewer provided comments that helped to improve the manuscript. This research was funded by the Critical Ecosystem Partnership Fund (CEPF) and Fondo de Promoción de las Áreas Naturales Protegidas del Perú (PROFONANPE), via APECO and CORBIDI with the projects Updating the status of an endemic harlequin frog from Peru (project number CEPF-108792) and Diversity and conservation status of the herpetofauna from Cordillera de Colán, Perú (project number CEPF-113268), respectively; Beca Carlos Ponce by APECO with the project Population assessment and ecology of Centrolene lemniscatum in Cordillera de Colán (project number N°006-2019-APECO); and Global Genome Initiative (GGBN-GGI) with the project Preserving treasures: saving the Peruvian herpetofauna genome.

References

BATALLAS, D. & J. BRITO (2016): Análisis bioacústico de las vocalizaciones de seis especies de anuros de la laguna Cormorán, complejo lacustre de Sardinayacu, Parque Nacional Sangay, Ecuador. – Revista Mexicana de Biodiversidad, 87: 1292–1300.

Bossuyt, F. & M. C. Milinkovitch (2000): Convergent adaptive radiations in Madagascan and Asian ranid frogs reveal covariation between larval and adult traits. – Proceedings of the National Academy of Sciences of the U.S.A., **97**: 6585–6590.

- CADLE, J. E. (1991): Systematics of lizards of the genus *Stenocercus* (Iguania: Tropiduridae) from northern Perú: New species and comments on relationships and distribution patterns. Proceedings of the Academy of Natural Sciences of Philadelphia, 143: 1–96.
- CADLE, J. E. (2001): A new species of lizard related to *Stenocercus caducus* (Cope) (Squamata: Iguanidae) from Peru and Bolivia, with a key to the "Ophryoessoides Group". Bulletin of the Museum of Comparative Zoology, 157: 183–221.
- Catenazzi, A. & P. J. Venegas (2012): Anfibios y Reptiles/Amphibians and Reptiles. pp. 106–117, 260–271, 348–365 in: Pitman, N., E. R. Inzunza, D. Alvira, C. Vriesendorp, D. K. Moskovits, A. Campo, T. Wachter, D. F. Stotz, S. S. Noningo, C. E. Tuesta & R. C. Smith (eds): Peru: Cerro de Kampankis. Rapid Biological and Social Inventories Report, 24, The Field Museum, Chicago.
- CDC-UNALM (2006): Análisis del Recubrimiento Ecológico del Sistema Nacional de Áreas Naturales Protegidas por el Estado.
 CDC-UNALM/TNC, Lima, Peru.
- CHIARI, Y., M. VENCES, D. R. VIEITES, F. RABEMANANJARA, P. BORA, O. RAMILIJAONA RAVOAHANGIMALALA & A. MEYER (2004): New evidence for parallel evolution of colour patterns in Malagasy poison frogs (*Mantella*). Molecular Ecology, 13: 3763–3774.
- CISNEROS-HEREDIA, D. F. & R. W. McDIARMID (2007): Revision of the characters of Centrolenidae (Amphibia: Anura: Athesphatanura), with comments on its taxonomy and the description of new taxa of glassfrogs. Zootaxa, 1572: 1–82.
- Dalapicolla, J. & A. R. Percequillo (2020): Species concepts and taxonomic practice in the integrative taxonomy era: an example using South American rodents. Boletim da Sociedade Brasileira de Mastozoologia, 88: 36–54.
- DE QUEIROZ, K. (1998): The general lineage concept of species, species criteria, and the process of speciation. pp. 57–75 in: HOWARD, D. J. & S. H. BERLOCHER (eds): Endless forms: species and speciation. Oxford University Press.
- DE QUEIROZ, K. (2007): Species concepts and species delimitation. Systematic Biology, **56**: 879–886.
- Duarte-Marín, S., M. Rada, M. Rivera-Correa, V. Caorsi, E. Barona, G. González-Durán & F. Vargas-Salinas (2022): Tic, Tii and Trii calls: advertisement call descriptions for eight glass frogs from Colombia and analysis of the structure of auditory signals in Centrolenidae. Bioacoustics, 32: 143–180.
- Duellman, W. E. (1999): Patterns of distribution of amphibians: a global perspective. John Hopkins University Press.
- FROST, D. R. (2025): Amphibian Species of the World: an Online Reference. Version 6.2 (accessed 19 September 2025). Electronic Database accessible at https://amphibiansoftheworld. amnh.org/index.php. – American Museum of Natural History, New York, USA.
- Funk, W. C., M. Caminer & S. R. Ron (2011): High levels of cryptic species diversity uncovered in Amazonian frogs. Proceedings of the Royal Society B, 279: 1806–1814.
- GOSNER, K. L. (1960): A simplified table for staging anuran embryos and larvae with notes on identification. Herpetologica, **16**: 183–190.
- Guayasamin, J. M., S. Castroviejo-Fisher, L. Trueb, J. Ayarzagüena, M. Rada & C. Vilà (2009): Phylogenetic systematics of glassfrogs (Amphibia: Centrolenidae) and their sister taxon *Allophryne ruthveni*. Zootaxa, **2100**: 1–97.

- Guayasamin, J. M., D. F. Cisneros-Heredia, R. W. McDiarmid, P. Peña & C. R. Hutter (2020): Glassfrogs of Ecuador: diversity, evolution, and conservation. Diversity, 12: 222.
- HAZZI, N. A., J. S. MORENO, C. ORTIZ-MOVLIAV & R. D. PALACIO (2018): Biogeographic regions and events of isolation and diversification of the endemic biota of the tropical Andes. Proceedings of the National Academy of Sciences of the U.S.A., 115: 7985–7990.
- Hrbek, T. & A. Larson (1999): The evolution of diapause in the killifish family Rivulidae (Atherinomorpha, Cyprinodontiformes): a molecular phylogenetic and biogeographic perspective. Evolution, 53: 1200–1216.
- Hutter, C. R., J. M. Guayasamin & J. J. Wiens (2013): Explaining Andean megadiversity: the evolutionary and ecological causes of glassfrog elevational richness patterns. Ecology Letters, **16**: 1135–1144.
- Kalyaanamoorthy, S., B. Q. Minh, T. K. F. Wong, A. Von Haeseler & L. S. Jermiin (2017): ModelFinder: fast model selection for accurate phylogenetic estimates. Nature Methods, 14: 587–589.
- KATOH, K. & D. M. STANDLEY (2013): MAFFT multiple sequence alignment software version 7: improvements in performance and usability. Molecular Biology and Evolution, 30: 772–780.
- Kocher, T. D., W. K. Thomas, A. Meyer, S. V. Edwards, S. Pää-Bo, F. X. Villablanca & A. C. Wilson (1989): Dynamics of mitochondrial DNA evolution in animals: amplification and sequencing with conserved primers. – Proceedings of the National Academy of Sciences of the U.S.A., **86**: 6196–6200.
- KÖHLER, J., F. GLAW, C. AGUILAR-PUNTRIANO, S. CASTROVIEJO-FISHER, J. C. CHAPARRO, I. DE LA RIVA, G. GAGLIARDI-URRUTIA, R. GUTIÉRREZ, M. VENCES & J. M. PADIAL (2024): Similar looking sisters: A new sibling species in the *Pristimantis danae* group from the southwestern Amazon basin (Anura, Strabomantidae). Zoosystematics and Evolution, 100: 565–582.
- Köhler, J., M. Jansen, A. Rodríguez, P. J. R. Kok, L. F. Toledo, M. Emmrich, F. Glaw, C. F. B. Haddad, M.-O. Rödel & M. Vences (2017): The use of bioacoustics in anuran taxonomy: theory, terminology, methods and recommendations for best practice. Zootaxa, 4251: 1–124.
- KÖHLER, J., P. J. VENEGAS, E. CASTILLO-URBINA, F. GLAW, C. AGUILAR-PUNTRIANO & M. VENCES (2023): A third species of glassfrog in the genus *Chimerella* (Anura, Centrolenidae) from central Peru, discovered by an integrative taxonomic approach. Evolutionary Systematics, 7: 195–209.
- KUMAR, S., G. STECHER & K. TAMURA (2016): MEGA7: Molecular Evolutionary Genetics Analysis Version 7.0 for Bigger Datasets. – Molecular Biology and Evolution, 33: 1870–1874.
- Luedtke, J. A., J. Chanson, K. Neam, L. Hobin, A. O. Maciel, A. Catenazzi, A. Borzée, A. Hamidy, A. Aowphol & A. Jean (2023): Ongoing declines for the world's amphibians in the face of emerging threats. Nature, 622: 308–314.
- Malcolm, J. R., C. Liu, R. P. Neilson, L. Hansen & L. E. E. Hannah (2006): Global warming and extinctions of endemic species from biodiversity hotspots. Conservation Biology, 20: 538–548.
- MARTIN, A. P. (1999): Substitution rates of organelle and nuclear genes in sharks: implicating metabolic rate (again). Molecular Biology and Evolution, 16: 996–1002.

- MATSCHINER, M. (2016): Fitchi: haplotype genealogy graphs based on the Fitch algorithm. Bioinformatics, 32: 1250–1252.
- McDiarmid, R. W. (1994): Preparing amphibians as scientific specimens. pp. 289–296 in: Heyer, W. R., M. A. Donnelly, R. W. McDiarmid, L.-A. C. Hayek & M. S. Foster (eds): Measuring and monitoring biological diversity. Standard methods for amphibians. Smithsonian Institution Press, Washington.
- Myers, N., R. A. Mittermeier, C. G. Mittermeier, G. A. da Fonseca & J. Kent (2000): Biodiversity Hotspots for conservation priorities. – Nature, 403: 853–858.
- NGUYEN, L.-T., H. A. SCHMIDT, A. VON HAESELER & B. Q. MINH (2015): IQ-TREE: A fast and effective stochastic algorithm for estimating maximum-likelihood phylogenies. Molecular Biology and Evolution, 32: 268–274.
- Ortega-Andrade, H. M., O. R. Rojas-Soto, J. H. Valencia, A. Espinosa de los Monteros, J. J. Morrone, S. R. Ron & D. C. Cannatella (2015): Insights from integrative systematics reveal cryptic diversity in *Pristimantis* frogs (Anura: Craugastoridae) from the upper Amazon Basin. PLoS One, 10: e0143392.
- Padial, J. M. & I. De la Riva (2009): Integrative taxonomy reveals cryptic Amazonian species of *Pristimantis* (Anura Strabomantidae). Zoological Journal of the Linnean Society, 155: 97–122.
- Padial, J. M., A. Miralles, I. De la Riva & M. Vences (2010): The integrative future of taxonomy. – Frontiers in Zoology, 7: 16.
- PÁEZ, N. B. & S. R. RON (2019): Systematics of *Huicundomantis*, a new subgenus of *Pristimantis* (Anura, Strabomantidae) with extraordinary cryptic diversity and eleven new species. ZooKeys, **868**: 1–112.
- Palumbi, S. R., A. Martin, S. Romano, W. O. McMillan, L. Stice & G. Grabowski (1991): The simple fool's guide to PCR, version 2.0. University of Hawaii, Honolulu, 45: 26–28.
- Peñaherrera del Aguila, C. (1989): Atlas del Perú. Instituto Geográfico Nacional, Lima.
- RODRIGUES, A. S. L., T. M. BROOKS, S. H. M. BUTCHART, J. CHANSON, N. COX, M. HOFFMANN & S. N. STUART (2014): Spatially explicit trends in the global conservation status of vertebrates. PLoS One, **9:** e113934.
- Ron, S. R., D. García, D. Brito-Zapata, C. Reyes-Puig, E. Figueroa-Coronel & D. F. Cisneros-Heredia (2024): A new glassfrog of the genus *Centrolene* (Amphibia, Centrolenidae) from the Subandean Kutukú Cordillera, eastern Ecuador. Zoosystematics and Evolution, **100**: 923–939.
- Scott, N. J. (1994): Complete species inventories. pp. 78–84 in: Heyer, W. R., M. A. Donnelly, R. W. McDiarmid, L. C. Hayek & M. S. Foster (eds): Measuring and monitoring biological diversity: standard methods for amphibians. Smithsonian Institution Press, Washinton.
- SHEN, X.-X., D. LIANG & P. ZHANG (2012): The development of three long universal nuclear protein-coding locus markers and their application to osteichthyan phylogenetics with nested PCR. – PLoS One, 7: e39256.
- SIMPSON, G. G. (1951): The species concept. Evolution, 5: 285–298.
- Sites Jr., J. W. & J. C. Marshall (2004): Operational criteria for delimiting species. Annual Review of Ecology Evololution and Systematics, 35: 199–227.

- STEPHENS, M., N. J. SMITH & P. DONNELLY (2001): A new statistical method for haplotype reconstruction from population data. The American Journal of Human Genetics, **68**: 978–989.
- Twomey, E., J. Delia & S. Castroviejo–Fisher (2014): A review of northern Peruvian glassfrogs (Centrolenidae), with the description of four new remarkable species. Zootaxa, 3851: 1–87.
- VENCES, M., J. KOSUCH, F. GLAW, W. BÖHME & M. VEITH (2003): Molecular phylogeny of hyperoliid treefrogs: biogeographic origin of Malagasy and Seychellean taxa and re-analysis of familial paraphyly. – Journal of Zoological Systematics and Evolutionary Research, 41: 205–215.
- VENCES, M., A. MIRALLES, S. BROUILLET, J. DUCASSE, A. FEDO-SOV, V. KHARCHEV, I. KOSTADINOV, S. KUMARI, S. PATMANIDIS & M. D. SCHERZ (2021): iTaxoTools 0.1: Kickstarting a specimen-based software toolkit for taxonomists. – BioRxiv: 2021– 2003.
- Vences, M., A. Miralles & C. Dufresnes (2024a): Next-generation species delimitation and taxonomy: implications for biogeography. Journal of Biogeography, 51: 1709–1722.
- VENCES, M., S. PATMANIDIS, V. KHARCHEV & S. S. RENNER (2022): Concatenator, a user-friendly program to concatenate DNA sequences, implementing graphical user interfaces for MAFFT and FastTree. – Bioinformatics Advances, 2: vbaco50.
- Vences, M., S. Patmanidis, J.-C. Schmidt, M. Matschiner, A. Miralles & S. S. Renner (2024b): Hapsolutely: a user-friendly tool integrating haplotype phasing, network construction, and haploweb calculation. Bioinformatics Advances, 4: vbaeo83.
- Venegas, P. J., L. A. García-Ayachi, J. C. Chávez-Arribasplata, A. Marchelie, S. Bullard, E. Quispe, J. D. Valencia, J. Odar & O. Torres-Carvajal (2024): Two new species of wood lizards (Hoplocercinae: *Enyalioides*) from Cordillera de Colán in north-eastern Peru. Journal of Vertebrate Biology, 73: 23074.
- WILEY, E. O. (1978): The evolutionary species concept reconsidered. Systematic Biology, 27: 17–26.
- WILL, K. W., B. D. MISHLER & Q. D. WHEELER (2005): The perils of DNA barcoding and the need for integrative taxonomy. Systematic Biology, **54**: 844–851.
- WINGER, B. M. & J. M. BATES (2015): The tempo of trait divergence in geographic isolation: Avian speciation across the Marañon Valley of Peru. – Evolution, 69: 772–787.